

## Band Gap Energy Modification of TiO<sub>2</sub> Photoelectrode By PbS/CdS Quantum Dot to Enhance Visible Region Photocurrent

Supriyono<sup>1\*</sup>, Yuni Krisyuningsih Krisnandi<sup>1</sup>, and Jarnuzi Gunlazuardi<sup>1</sup>

<sup>1</sup>Department of Chemistry, Faculty of Mathematic and Sciences, University of Indonesia, Kampus Baru UI Depok, Depok 16424, Indonesia

**Abstract :** TiO<sub>2</sub> nanoparticles co-sensitized by CdS and PbS quantum dots (QD) were successfully prepared by a two-step process of sol gel method followed by successive ionic layer adsorption and reaction (SILAR) technique. Optical band gap energy and the particle size of the QD were determined from UV-Vis DRS spectra by using Tauc method and Brus model, respectively. XRD patterns indicated that the TiO<sub>2</sub> nanoparticles have a nano-size crystallite range of 20-50 nm, while the DRS analysis showed that the optical band gap of TiO<sub>2</sub> and CdS were 3,34 eV and 2,38 eV, respectively. The diameter of CdS QD calculated by Tauc and Yu equation was around 9 nm. The shifted of optical band gap from UV to visible region was used to monitor the enhancement of visible photocurrent. Photoelectrochemical test showed that the TiO<sub>2</sub> (E<sub>g</sub> = 3.34 eV) generated a photocurrent in the visible region of 0.01 mA/cm<sup>2</sup> and after TiO<sub>2</sub> coated by CdS (E<sub>g</sub> = 2.38 eV) its photocurrent increased to 0.30 mA/cm<sup>2</sup>. The results showed that the PbS/CdS co-sensitization have successfully enhanced the performance of TiO<sub>2</sub> photoelectrode by improving visible light adsorption efficiency and electron transport rate. We believe that this sensitizers and proposed structure have good prospects for photovoltaic development in the future.

**Keywords:** Optical bandgap, photoelectrochemical, quantum dot, sensitizer, TiO<sub>2</sub>.

### Introduction

The use of fossil fuels has been viewed as a major environmental threat because of their substantial contribution to greenhouse gases. These conditions encourage many researchers to harness the sun's energy which could not just solve the present energy problem but also fulfill our future demand. As one hour solar energy can be used for one year, therefore, we only need to harvest less than 0.02 of solar energy<sup>1</sup>. There are many researches for solving our energy problems and among the renewable energy sources, solar cells have attracted a great interest as a solution to this situation<sup>2,3</sup>. Today, the silicon-based photovoltaic devices have power-conversion efficiencies over 20%<sup>4</sup>. However, the issues of high cost and environmentally-harmful waste in the processing technologies of silicon-based solar cells should be resolved<sup>5</sup>. Dye-sensitized solar cells (DSSCs) invented by Michael Grätzel became a very popular alternative to silicon based solar cells because of their great potential to convert solar energy into electric energy at low cost<sup>6,7</sup>. This cell can be made from cheap materials such as inorganic and organic dyes which do not need to be highly pure as is required for silicon solar cell<sup>8</sup>. A typical DSSC consist sofa working electrode (photoanode) and acounter electrode(CE) separated by as altelectrolyte<sup>9</sup>. Photo anode consists of a mesoporous wide band gap semiconductor (TiO<sub>2</sub>) layer that is attached to the conducting glass. Titanium dioxide (TiO<sub>2</sub>) has been extensively used as a photo anode for quantum dot

sensitized solar cells (QDSSCs) because of its favorable band-edge positions, strong optical absorption, good chemical stability, photocorrosion resistance, and low cost. However, its large band gap (3.2 eV) means that TiO<sub>2</sub> can only harvest UV light, which is just 5% of sunlight, resulting in low energy conversion efficiency. Much effort has been made to improve its visible light harvesting ability. One of the strategies that is widely employed in QDSSCs, is sensitizing TiO<sub>2</sub> with multiple narrow band gap semiconductors such as CdS, and PbS<sup>10</sup>. Among the various QD materials, CdS has been receiving much attention because of its high potential in photoabsorption in the visible region. However, CdS semiconductors only absorb visible light with the energy more than 2.4 eV, and visible light with wavelength longer than 520 nm cannot be absorbed. PbS is regarded as a promising material for solar energy due to its band gap (E<sub>g</sub> = 0.41 eV) which covers the range of the solar spectrum. Therefore, combination of rapid electron injection rate by CdS nanoparticles and wide visible light absorption area by PbS nanoparticles could enhance the charge separation and extend the absorption response to the entire visible region<sup>11</sup>.

In this study, we prepared TiO<sub>2</sub> photoelectrode and sensitized them by multiple quantum dots, which are PbS and CdS. The effects of the deposition of quantum dots (PbS, CdS) to the generated photocurrent were investigated. The relationships between visible photocurrent enhancement and optical band gap shift will be studied and discussed herein.

## Methodology

All chemicals and solvents used in this research were of reagent grade. Titanium (IV) isopropoxide (TTIP), polyethylene glycol (PEG, Mr = 1000), triethanolamine were purchased from Sigma Aldrich. While methanol, ethanol, Cd(CH<sub>3</sub>COO)<sub>2</sub>·2H<sub>2</sub>O, Na<sub>2</sub>S·9H<sub>2</sub>O, Pb(NO<sub>3</sub>)<sub>2</sub> were purchased from Merck. Distilled water produced from a BioPure purification system was used throughout the experiments and homemade fluor doped tin oxide (FTO) with the sheet resistance = 21Ω/sq<sup>12</sup>.

### 1. Preparation of FTO/TiO<sub>2</sub> film

TiO<sub>2</sub> sol was prepared by mixing of 7.5 mL TTIP, 2.4 mL triethanolamine, and 36 mL of ethanol. The mixture was stirred with a magnetic stirrer at room temperature for 1.5 hours, then was added by adequate ethanol-water (4.5mL:0.5mL) and 2 grams of PEG, and stirred for 1.5 hours. The resulted sol then was used to coat the FTO glass by a dip coating method, and then annealed at 500°C for 1 hour. This step was repeated for 5 times.

### 2. Preparation of FTO/TiO<sub>2</sub>/CdS film

CdS quantum dot (QD) was prepared by successive ionic layer adsorption and reaction (SILAR) method. Individual solution containing Cd(CH<sub>3</sub>COO)<sub>2</sub> and Na<sub>2</sub>S were used as a Cd and S precursor, respectively. The CdS was deposited directly by immersing the FTO/TiO<sub>2</sub> glass into the solution of Cd(CH<sub>3</sub>COO)<sub>2</sub> 0.3M for 2 minutes, then rinsed with distilled water. Then was immersed in the solution of Na<sub>2</sub>S 0.3M for 2 minutes, then rinsed with distilled water. This step was repeated 10 times until the optimum CdS layer was formed.

### 3. Preparation of FTO/TiO<sub>2</sub>/PbS/CdS film

PbS was prepared by a SILAR method. The FTO/TiO<sub>2</sub> was soaked in the solution of Pb(NO<sub>3</sub>)<sub>2</sub> 0,02M in methanol for 2 minutes and then rinsed with ethanol. Then was soaked in a solution of Na<sub>2</sub>S 0,02M in methanol: water (1:1) for 5 minutes, then rinsed with ethanol. This step was performed up to 3 cycles in order to obtain desired thickness. Then proceeded by the CdS layer in the same manner as above.

### 4. Characterizations

Characterization of the film structure was done by using X-ray diffractometer (Shimadzu XRD 7000) with CuKα radiation (λ = 1.5418 Å), at 30 kV, 10 mA. The surface morphology of the film surface was observed with field emission scanning electron microscope (FESEM, FEI-Inspect F50) and composition of the constituent elements measured by Energy Dispersive Spectroscopy (EDS) Apollo X. Optical band gap was obtained from UV-Vis diffuse reflectance spectra that were recorded by UV-Vis diffuse reflectance spectrophotometer (DRS) Simadzu UV2450. Generated photocurrent was measured using an electrochemical

workstation (e-DAQ/e-recorder 401) using 60W wolfram lamp as visible light source (with the intensity 2.2 mW/cm<sup>2</sup>) and Na<sub>2</sub>S 0.3M solution as electrolyte.

## Results and Discussion

### 1. Structural and morphological studies

Figure 1 showed the XRD patterns of the FTO, FTO/TiO<sub>2</sub>, and FTO/TiO<sub>2</sub>/PbS/CdS films. The XRD pattern from figure 1a showed that the FTO substrates have a cassiterite structure (JCPDS no.41-1445).As shown in Figure 1b, besides the diffraction peaks from cassiterite on structured SnO<sub>2</sub>, the other peaks could be indexed as the (101), (004), and (200) planes of tetragonal anatase structure TiO<sub>2</sub> (JCPDS no.21-1272).

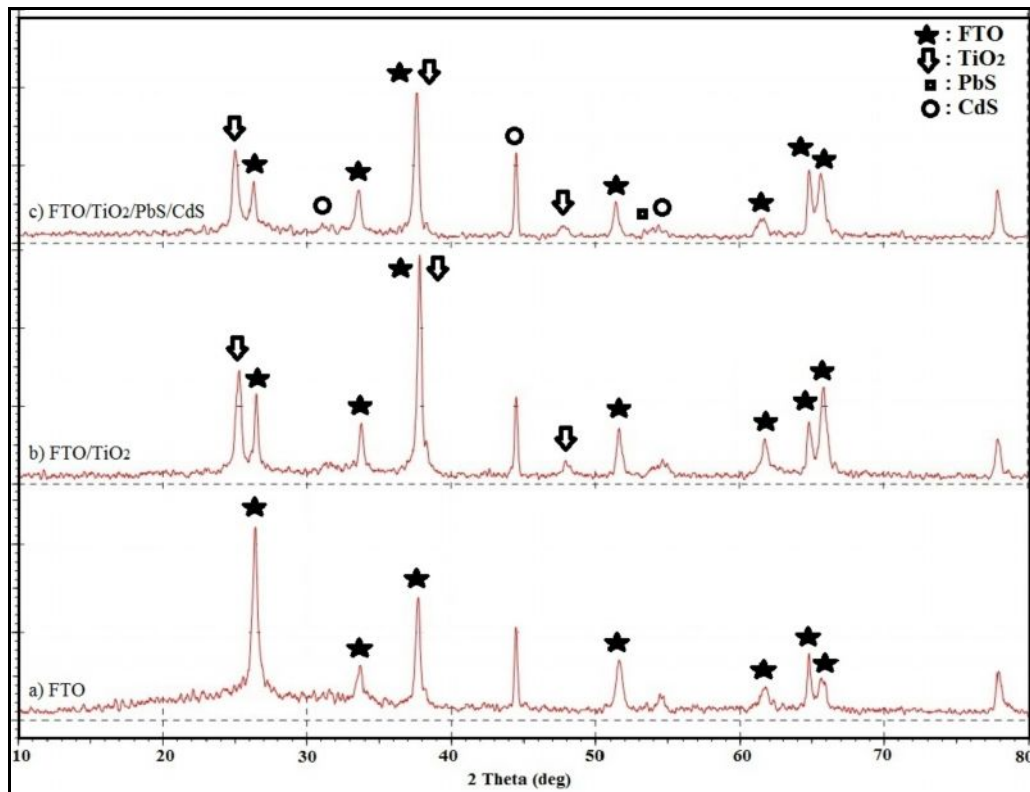


Figure 1. X-ray diffraction patterns of a) FTO, b) FTO/TiO<sub>2</sub>, c) FTO/TiO<sub>2</sub>/PbS/CdS films

Meanwhile, due to small quantities of PbS and CdS, so after PbS/CdS was deposited on the surface of TiO<sub>2</sub>, it didn't show any clear new peaks. PbS and CdS only appeared as a small peak, and allowed the other peaks that overlap with existing peak of FTO and TiO<sub>2</sub>. It was also probably because of PbS and CdS only dried at room temperature without any calcination so it was possible that the PbS and CdS still amorphous, so that the resulted peaks were small and broad. According to Balaz *et al.*, 2003<sup>13</sup>, CdS had two structures, these were hexagonal  $\alpha$ -CdS called greenockite (JCPDS 41-1049) and cubic  $\beta$ -CdS called hawleyite (JCPDS 10-0454), while PbS had only galena structure (JCPDS 05-0592). The XRD pattern from figure 1c showed that CdS had three peaks corresponding to (200), (220), and (311) planes of cubic  $\beta$ -CdS (hawleyite) at  $2\theta$  values of 31.1°, 44.5°, and 51.8°, respectively, while PbS showed one broad peak at  $2\theta$  values of 53.4° identified to be due to reflections from (222) planes of cubic PbS (galena). The crystallite size of TiO<sub>2</sub> was estimated using the following Scherrer equation<sup>14</sup>:

$$D = k\lambda / (\cos\theta)$$

1)

where the constant  $k$  is a shape factor usually  $\sim 0.9$ ,  $\lambda$  is the wave length of X-ray (0.15418 nm),  $\beta$  is the full width at half maximum(FWHM) in radians and  $\theta$  is the Bragg's angle. The estimation showed that the mean crystallite size of the anatase  $\text{TiO}_2$  particles calculated from Scherrer equation was 20–50 nm.

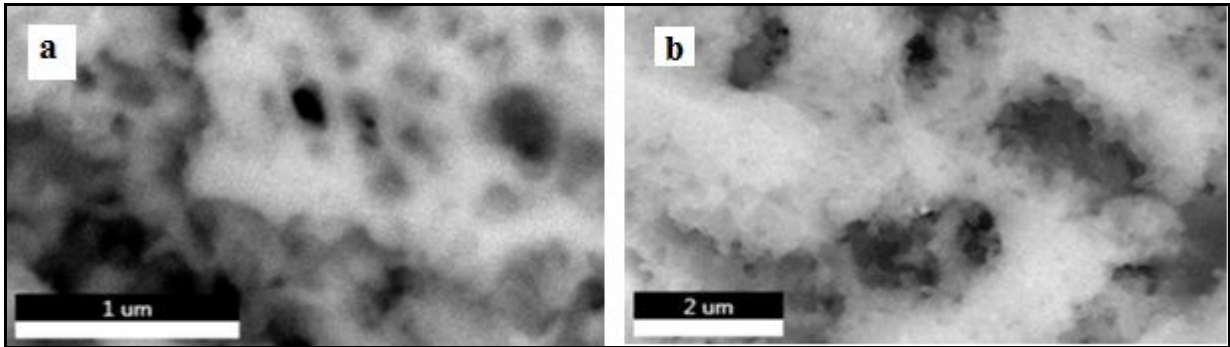


Figure 2. FESEM images of FTO/ $\text{TiO}_2$  layer a) before, b) after coated by PbS/CdS QD

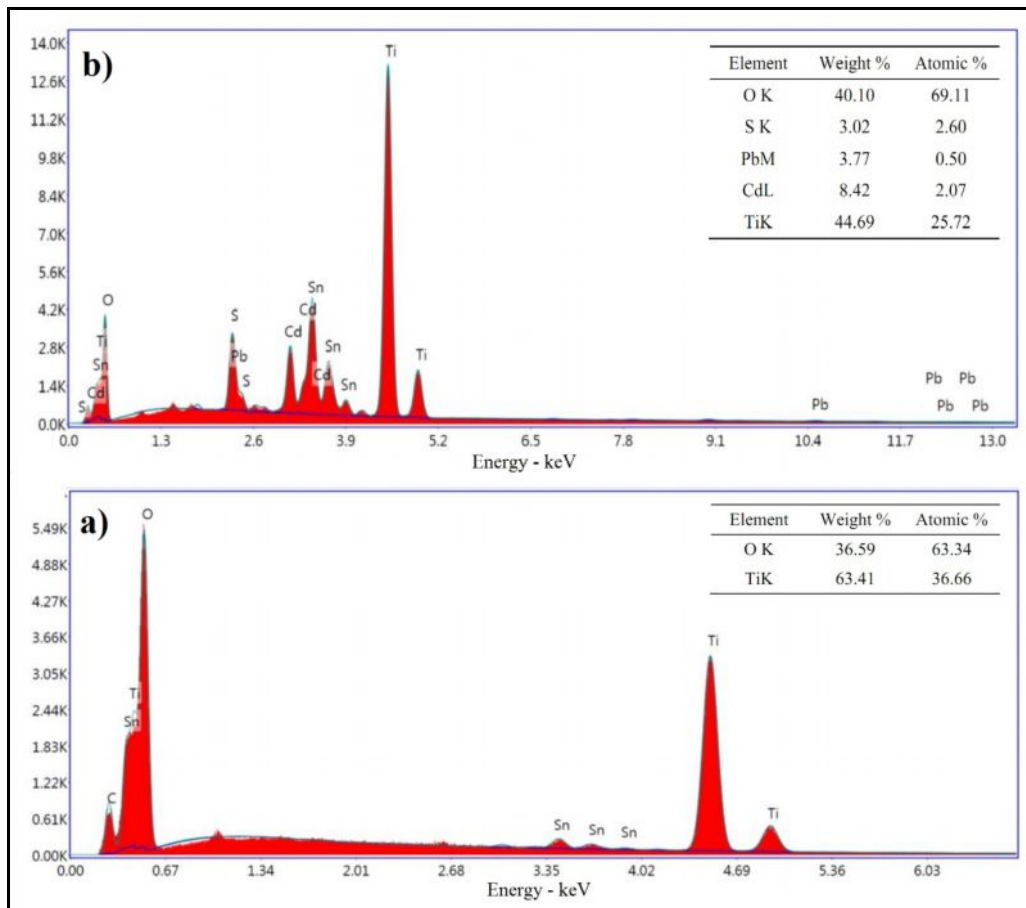


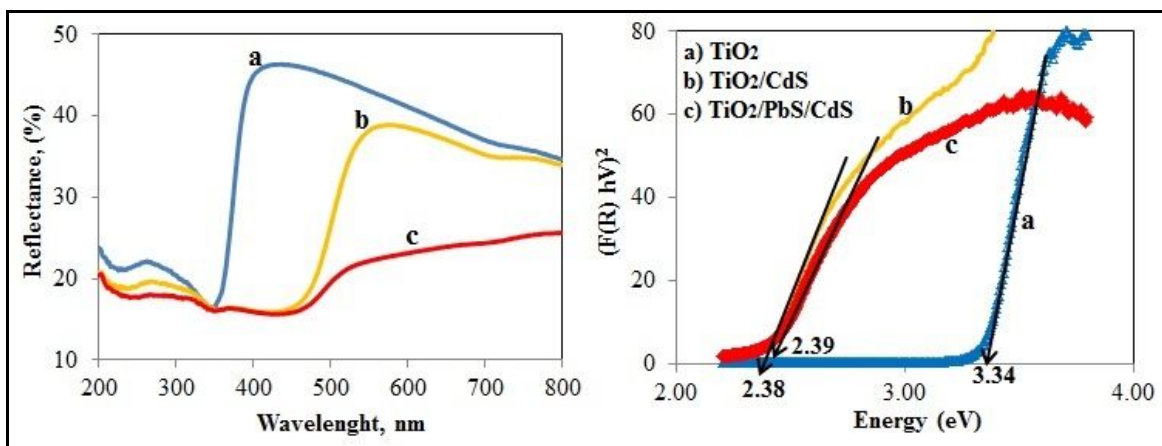
Figure 3. EDS spectra and elemental composition of a) FTO/ $\text{TiO}_2$  and b) FTO/ $\text{TiO}_2$ /PbS/CdS films

Figure 2a showed the typical FESEM images of  $\text{TiO}_2$  nanoparticles on the FTO-coated glass substrate, confirming that the FTO-coated glass substrate was uniformly covered with ordered  $\text{TiO}_2$  nanoparticles. Figure 2b showed  $\text{TiO}_2$  nanoparticles was coated by PbS/CdS QD. These results were confirmed by EDS spectra in Figure 3. Before  $\text{TiO}_2$  was coated by CdS, there were only a constituent element of titanium (Ti) and oxygen (O), but after being coated by PbS/CdS, it appeared all the constituent elements with the content of each 44.69% Ti, 40.10% O, 8.42% cadmium (Cd), 3.77% lead (Pb), and 3.02% sulphur (S). This indicated that PbS and CdS had successfully synthesized and deposited on the surface of  $\text{TiO}_2$ . Based on EDS spectra in Figure 3a, the elemental composition of titanium (Ar = 48) was 63.41% (1.3 mole) and oxygen (Ar = 16) was 36.59% (2.3 mole). From the mole ratio of Ti and O = 1: 2, it was confirmed that the compound was  $\text{TiO}_2$ . While based on

the EDS spectra in Figure 3b, in addition to the elements Ti and O, there was also an element of cadmium (Ar = 112) as much as 8.72% (0.075 mole), sulphur (Ar = 32) as much as 3.02% (0.093 mole), and lead (Ar = 207) as much as 3.77% (0.018 mole). Mole ratio of S in the compounds of CdS and PbS was 1: 1. The formation of CdS compound needed 0.075 mole S, so there was remaining S as much as 0.018mole, and this rest of mole S was used to bind with Pb, forming compound of PbS.

## 2. Optical band gap and particle size determination

The UV–Vis diffuse reflectance spectra (DRS) were used to find the optical band gap of the FTO/TiO<sub>2</sub>, FTO/TiO<sub>2</sub>/CdS and FTO/TiO<sub>2</sub>/PbS/CdS films. Figure4(left) showed that FTO/TiO<sub>2</sub>spectrum exhibited a strong absorption edge at around 380 nm. This UV–Vis DRS indicated that the excitation occurred on the UV light irradiation. And after it was coated by CdS or PbS/CdS, the strong absorption edge moved to wavelength of around 520 nm. Hence, it indicated that the excitation of the FTO/TiO<sub>2</sub>/CdS and FTO/TiO<sub>2</sub>/PbS/CdS films shift to the visible light irradiation.



**Figure 4. Left: DRS spectra ; Right: Optical band gap energy curve of TiO<sub>2</sub>, TiO<sub>2</sub>/CdS, and TiO<sub>2</sub>/PbS/CdS films**

The band gap energy of the TiO<sub>2</sub>, TiO<sub>2</sub>/CdS and TiO<sub>2</sub>/PbS/CdS films were evaluated using Kubelka–Munk F(R) function<sup>15,16</sup>.

$$F(R) = \frac{(1 - R)^2}{2R} = \frac{\alpha}{S} \quad 2)$$

The determination of optical band gap was obtained by Tauc's equation<sup>17</sup>.

$$\alpha h v = A(hv - E_g)^n \quad 3)$$

Where, R is the reflectance,  $\alpha$  is the absorption coefficient, S is the scattering coefficient, A is a constant that depends on the properties of the material,  $h\nu$  is the energy of the incident photons, h is Planck's constant,  $\nu$  is the frequency of the photon,  $E_g$  is the optical band gap, and n is a constant value that depends on the transition type;  $n = 1/2, 3/2$  for allowed and forbidden direct transition,  $n = 2, 3$  for allowed and forbidden indirect transition, respectively. The optical band gap energy was determined by plotting  $(F(R)hV)^2$  vs  $hV$ , as shown in Figure4 (right). The extrapolation of  $(F(R)hV)^2$  vs  $hV$  to zero would result in  $E = E_g$  and gavethe band gap energy of 3,34eV, 2,38eV and 2,39eV for TiO<sub>2</sub>, TiO<sub>2</sub>/CdS and TiO<sub>2</sub>/PbS/CdS films, respectively. It shown that the deposition of CdS and PbS QDs into TiO<sub>2</sub> can shift its optical absorption edge from UV into visible light range.

The size of the QDs can be estimated using the following Brus equation<sup>18</sup>.

$$\Delta E = E1 - Eg = \left( \frac{h^2}{8r^2} \right) \left( \frac{1}{m_e} + \frac{1}{m_h} \right) \quad 4)$$

Where  $\Delta E$  is the band gap energy shift,  $E1$  is the band gap of the QD,  $Eg$  is the band gap of the bulk materials,  $r$  is the radius of the QD,  $h$  is the Plank's constant, and  $m_e$  and  $m_h$  are the effective masses of the electron and hole, respectively. For CdS material,  $m_e = 0.19m_0$ ,  $m_h = 0.80m_0$  ( $m_0 = 9.11 \times 10^{-31}$  kg), and  $Eg = 2.25\text{eV}$ <sup>19</sup>. The estimation showed that the diameter of CdSQD calculated from Brus equation was 8.6 nm. In addition of Brus equation, the size of the QD can also be estimated using Yu equation. Yu model is an empirical relationship between the wavelength value corresponding to the  $Eg$  and the particle diameter ( $D$ ), for CdS QD expressed as:<sup>20</sup>

$$D = -6.6521 \times 10^{-8} \lambda^2 + 1.9557 \times 10^{-4} \lambda^2 - 9.2352 \times 10^{-2} \lambda + 13.29 \quad 5)$$

According to Zhang et al., 2009<sup>21</sup>, the energy band gap ( $Eg$ ) of CdS nanoparticles can be calculated using equation 6:

$$Eg = \frac{1240}{\lambda} \quad 6)$$

The diameter estimation of CdSQD calculated by Yu equation was 8.9nm. Detailed calculation of the QD diameter by using both equations, can be seen in Table 1. Generally, QDs are extremely small semiconductor nano crystals with a size comparable to the Bohr radius of an exciton. For most semiconductors, the Bohr radius of an exciton was in the range of 1 – 10 nm<sup>22</sup>.

**Table 1. Diameter of quantum dots, estimated by Brus equation and Yu equation**

Type of QDs	Band gap of bulk CdS ( $Eg$ ), eV	Band gap of QD ( $E1$ ), eV	Wavelength of QD, nm ( $\lambda=1240/E1$ )	Diameter of QD, nm (Brus eq.)	Diameter of QD, nm (Yu eq.)
CdS	2.25	2.38	521	8.6	8.9
PbS/CdS	2.25	2.39	519	8.4	8.7

### 3. Photocurrent response study

According to Jiao et al., 2013<sup>23</sup>, there are three strategies to improve the performance of solar cell: by improving light harvesting efficiency, the electron transport rate, and decrease the degree of charge recombination. Figure 4 shown that  $\text{TiO}_2$  absorb mainly the ultraviolet light with a wavelength below 400 nm. After the deposition of CdS QD, the absorption edge is shifted significantly toward the visible region with a band edge of 520 nm. Further sensitization by PbS/CdS QD can absorb all the visible light in the solar spectrum, making it a promising sensitizer for solar cell applications. As shown in Figure5a that photocurrent responses of the FTO/ $\text{TiO}_2$ , FTO/ $\text{TiO}_2$ /CdS and FTO/ $\text{TiO}_2$ /PbS/CdS electrodes measured under visible-light irradiation were 0,01 mA/cm<sup>2</sup>, 0.19 mA/cm<sup>2</sup> and 0.30 mA/cm<sup>2</sup>, respectively. FTO/ $\text{TiO}_2$  electrode didn't show any obvious enhancement in visible photocurrent because of poor visible light absorption. After  $\text{TiO}_2$  sensitized by PbS/CdS QD, the band gap shifted to visible region. Our results indicated that the high photocurrent of FTO/ $\text{TiO}_2$ /PbS/CdS electrode was attributed to the high visible light harvesting efficiency and the effective electron transport rate from the conduction band QD to conduction band  $\text{TiO}_2$ . Figure 5b shown that by coupling two narrow bandgap semiconductors, such as CdS and PbS, was possible to maximize the efficiency of charge separation. The matched of the conduction and valence bands of the two semiconductors, allowed the accumulation of electrons and holes in two separate particles, thus allowing enough time to capture one of the charge carriers at the electrode surface

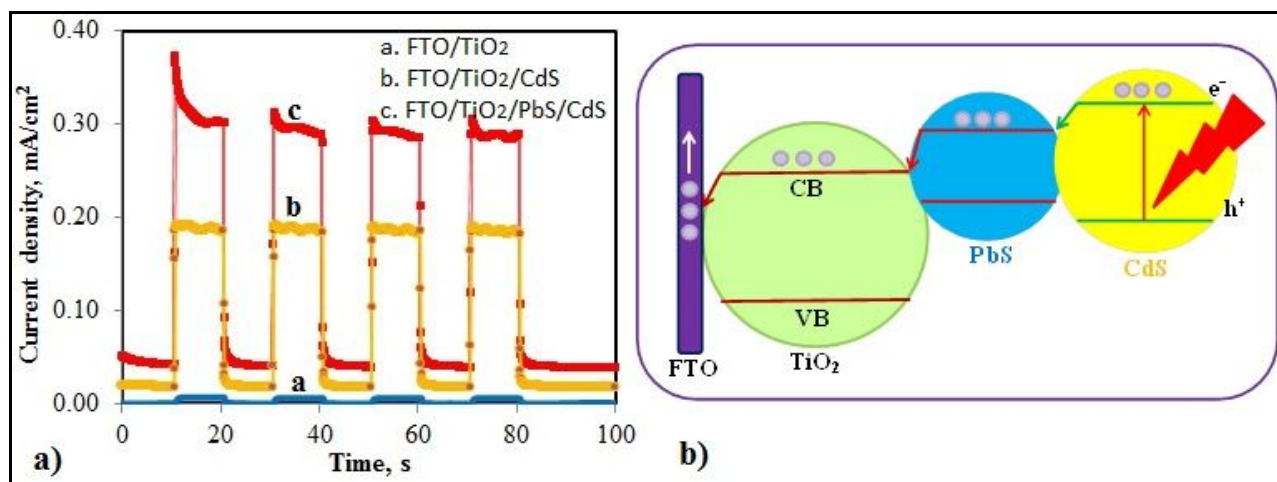


**Figure 5 a) Photocurrent of FTO/TiO<sub>2</sub>, FTO/TiO<sub>2</sub>/CdS and FTO/TiO<sub>2</sub>/PbS/CdS photoelectrode, b) Illustration of the electron transport mechanism in FTO/TiO<sub>2</sub>/PbS/CdS photoelectrode**

PbS with narrow band gap energy could be easily excited by visible light with low energy and induced the generation of electron hole pairs. However, the conduction of bulk PbS is more positive than TiO<sub>2</sub>, and the electron transfer from conduction band of PbS to TiO<sub>2</sub> would be inhibited. Fortunately, the quantum effect of PbS QD could change conduction band location. The nano-size of the PbS QD could cause the split of the conduction band, so the location could be more negative than TiO<sub>2</sub>, and the electron injection was occurred from the photo excited of PbS QD into the conduction band of TiO<sub>2</sub>. Hence, the electrons were collected from CdS and transferred across the interface of PbS, and then transferred to the surface of the TiO<sub>2</sub> nanoparticles. The electrons then traveled along the TiO<sub>2</sub> nanoparticles, passed through the interface between TiO<sub>2</sub>-FTO to the external circuit. The detailed mechanism about the electron transport of FTO/TiO<sub>2</sub>/PbS/CdS photoelectrode was illustrated in Figure 5b

## Conclusion

PbS and CdS QD for sensitizing TiO<sub>2</sub> photoelectrode have successfully prepared by SILAR method. Optical band gap and particle size of QD was determined by using UV-Vis DRS spectra and got the optical band gap of 3.34eV, 2.38eV, 2.39eV for TiO<sub>2</sub>, TiO<sub>2</sub>/CdS and TiO<sub>2</sub>/PbS/CdS, respectively. Particle size of the QD was calculated by using Tauc and Yu equation, with the result around 9 nm which is comparable with their Bohr radius. The shifted of optical band gap from UV to visible region can be used to monitor the enhancement of visible photocurrent. CdS and PbS QDs as co-sensitizers were successfully enhancing the performance of TiO<sub>2</sub> photoelectrode by improving light harvesting efficiency and electron transport rate. We believed that this sensitizers and proposed configuration have good prospects for photovoltaic development in the future.

## Acknowledgement

One of the authors (Supriyono) wishes to thank to Industrial Education and Training Center, Ministry of Industry of Indonesia for providing the scholarship and research funding. Partial support from Research Cluster Scheme University of Indonesia, (Titania Photo Electro Catalysis, (TIPEC) Cluster Research (contract number: 1864/UN2.R12/ HKP.05.00/2015)] is also acknowledged.

## References

1. Hammarstrom L, and Hammes-Schiffer S. Artificial Photosynthesis and Solar Fuels. *Acc. Chem.Res.*, 2009, 42: 1859-1860.
2. Kamat P.V. Meeting the Clean Energy Demand: Nanostructure Architectures for Solar Energy Conversion. *J. Phys. Chem. C.*, 2007, 111: 2834-2860.

3. Barnham KWJ, Mazzer M, and Clive B. Resolving the Energy Crisis: Nuclear or Photovoltaics. *Nat. Mater.*, 2006, 5: 161-164.
4. Saga T. Advances in Crystalline Silicon Solar Cell Technology for Industrial Mass Production. *NPG Asia Mater.*, 2010, 2: 96-102.
5. Ooyama Y, and Harima Y. Molecular Designs and Syntheses of Organic Dyes for Dye-Sensitized Solar Cells. *Eur. J. Org. Chem.*, 2009, 2903-2934.
6. Oregan B, and Grätzel M. A Low-cost, High-efficiency Solar-Cell Based on Dye-Sensitized Colloidal TiO<sub>2</sub> Films. *Nature*, 1991, 353: 737-740.
7. Gratzel M. Recent Advances in Sensitized Mesoscopic Solar Cells. *Acc. Chem. Res.*, 2009, 42: 1788-1798.
8. Hardin BE, Snaith HJ, and McGehee MD. The Renaissance of Dye-Sensitized Solar Cells. *Nat. Photon*, 2012, 6: 162-169.
9. Gratzel M. Conversion of Sun Light to Electric Power by Nanocrystalline Dye-Sensitized Solar Cells. *J. Photochem. and Photobiol. A: Chemistry*, 2004, 164:3-14.
10. Chen Y, Tao Q, Fu W, Yang H, Zhou X, Su S, Ding D, Mu Y, Lia X, and Lia M. Enhanced Photoelectric Performance of PbS/CdS Quantum Dot Co-Sensitized Solar Cells via Hydrogenated TiO<sub>2</sub> Nanorod Arrays. *Chem. Commun.*, 2014, 50: 9509-9512.
11. Acharya S, Das B, Thupakula U, Ariga K, Sarma DD, Israelachvili J, and Golan Y. A Bottom-up Approach Toward Fabrication of Ultrathin PbS Sheets. *Nano Lett.*, 2013, 13:409.
12. Supriyono, Surahman H, Krisnandi YK, and Gunlazuardi J. Preparation and Characterization of Transparent Conductive SnO<sub>2</sub>-F Thin Film Deposited by Spray Pyrolysis: Relationship Between Loading Level and Some Physical Properties. *Procedia Environmental Sciences*, 2015, 28: 242 – 251
13. Balaz P, Boldizarova E, Godocikova E, and Briancin J. Mechanochemical Route for Sulphide Nanoparticles Preparation. *Mater. Lett.*, 2003, 57: 1585-1589
14. Cullity BD. *Element of X-ray Diffraction*. Addison-Wesley Publication Company, Massachusetts, 1978
15. Sakhya AP, Dutta A, Shannigrahi S, and Sinha TP. Electronic Structure and Optical Properties of Orthorhombic and Rhombohedral RAlO<sub>3</sub>. *Solid State Sciences*. 2015, 42: 37-44.
16. Carrasco GF, Lopez JC, Martinez RM, Torres NDE, Munoz L, Milosevic O, and Rabanal ME. Optical and Morpho-Structural Properties of ZnO Nanostructured Particles Synthesized at Low Temperature via Air-Assisted USP Method. *Appl. Phys. A*, 2016, 122:173
17. Tauc J, Grigorovici R, and Vancu A. Optical Properties and Electronic Structure of Amorphous Germanium. *Phys. Stat. Sol.* 1966, 15(2): 627-637
18. Jun H.K, Careem MA, and Arof AK. Fabrication, Characterization, and Optimization of CdS and CdSe Quantum Dot-Sensitized Solar Cells with Quantum Dots Prepared by Successive Ionic Layer Adsorption and Reaction. *Int. J. Photoenergy*, 2014, Article ID 939423
19. Gratzel M. Photoelectrochemical cells. *Nature*, 2001, 414(6861): 338–344.
20. Yu WW, Qu L, Guo W, and Peng X. Experimental Determination of the Extinction Coefficient of CdTe, CdSe, and CdS Nanocrystals. *Chem. Mater.*, 2003, 15: 2854-2860.
21. Zhang X, Lei L, Zhang J, Chen Q, Bao J, and Fang B. A Novel CdS/S-TiO<sub>2</sub> Nanotubes Photocatalyst with High Visible Light Activity. *Separation and Purification Technology*. 2009, 66: 417–421
22. Tian J, and Cao G. Semiconductor Quantum Dot-Sensitized Solar Cells. *Nano Reviews*, 2013, 4:22578
23. Jiao J, Zhou ZJ, Zhou WH, Wu SX. CdS and PbS quantum dots co-sensitized TiO<sub>2</sub> nanorod arrays with improved performance for solar cells application. *Materials Science in Semiconductor Processing*, 2013, 16: 435-440

\*\*\*\*\*